

Limits on the precision of geobarometry at low grossular and anorthite content

CLIFFORD S. TODD*

Department of Geology and Geophysics, SOEST, University of Hawaii, Honolulu, Hawaii 96822, U.S.A.

ABSTRACT

In many cases the grossular content of garnet and/or the anorthite content of the plagioclase used in thermobarometry are very low, leading to a large pressure uncertainty. The dependence of this uncertainty on mole fractions of grossular and anorthite is evaluated by propagating uncertainties in composition and activity terms into the GASP geobarometer for a series of hypothetical rocks equilibrated at 550 °C and 6 kbar. Results are ± 0.65 kbar (1 standard deviation) at high mole fractions ($X_{\text{grs}} = 0.15$, $X_{\text{an}} = 0.98$), increasing to ± 1.55 kbar at low mole fractions ($X_{\text{grs}} = 0.03$, $X_{\text{an}} = 0.133$). Specific results vary depending on errors chosen, P - T conditions, thermodynamic database, and activity models used, but an overall trend of increasing uncertainty with decreasing mole fraction is robust. These theoretical conclusions are supported by a data set of 42 amphibolite facies metapelitic samples for which pressure and temperature were determined with and without grossular-anorthite-bearing equilibria. If grossular and anorthite mole fractions are large the difference in P determination is low (<0.5 kbar), but if these mole fractions are <0.10 and 0.30 , respectively, the difference in P determination is variable and can be high (>3 kbar). A general guideline is that if the product of grossular and anorthite mole fraction is <0.05 , then grossular-anorthite-bearing equilibria should be used only with great caution.

INTRODUCTION

Geothermometers and geobarometers are routinely used by geologists to estimate the pressure (P) and temperature (T) of equilibration of mineral assemblages. The uncertainties associated with these P - T estimates come from several sources, including experimental apparatus calibration, activity models, thermodynamic databases, P - T averaging technique, and mineral composition uncertainty. The effect of these uncertainties on the P - T estimate, either separately or in various combinations, has been investigated by several authors (Anderson 1977a, 1977b; Hodges and Crowley 1985; Hodges and McKenna 1987; McKenna and Hodges 1988; Powell and Holland 1988; Berman 1991; Kohn and Spear 1991a, 1991b; Lieberman and Petrakakis 1991; Gordon 1992; Applegate and Hodges 1994; Gordon et al. 1994; Powell and Holland 1994). None of the previous works systematically investigated the effects of low mole fraction of end-member components on the uncertainty of a P - T estimate, which is the purpose of this study. Two sources of uncertainty that vary with mole fraction are examined: uncertainties inherent in activity models and uncertainties in the compositions of minerals in the equilibrium assemblage.

For common assemblages in medium-grade metapelitic rocks, the problem of low mole fraction affecting P - T results is most acute for grossular-anorthite-bearing equilibria. Three commonly used equilibria are: Garnet-Alu-

minosilicate-silica-Plagioclase (GASP), $3 \text{ An} = \text{Gr}_s + 2 \text{ Al}_2\text{SiO}_5 + \text{Qtz}$ (Ghent 1976); Garnet-Rutile-Ilmenite-Plagioclase-Silica (GRIPS), $\text{Gr}_s + 2 \text{ Alm} + 6 \text{ Rt} = 6 \text{ Ilm} + 3 \text{ Qtz} + 3 \text{ An}$ (Bohlen and Liotta 1986), and Garnet-Mica-Aluminosilicate-Plagioclase (GMAP), $\text{Gr}_s + \text{Alm} + \text{Ms} = \text{Ann} + 3 \text{ An}$ (Ghent and Stout 1981). In many metapelites the mole fraction of grossular in garnet is $<10\%$. There are cases in which these equilibria have been used to estimate P - T conditions with X_{grs} below 2%. In typical metapelitic rocks, the anorthite component of plagioclase is commonly less than 30%. Certainly, there is a limit to how well activity models extrapolate to extremely low mole fractions. It is the purpose of this paper to investigate “how low is too low” without comparing different solution models, thermodynamic databases, or P - T averaging techniques. Consequently, a single choice of these parameters is used. The results presented here depend on the exact choice of these options. However, the conclusions regarding the functional relationship between mole fraction and the uncertainty of barometry should stand regardless of which database or solution model is preferred.

THEORETICAL CALCULATIONS

Uncertainty in activity model

As more experimental data are generated, activity models for minerals evolve and improve, and discrepancies among the most up-to-date models will likely decrease. However, low mole fractions are commonly outside the range of experiments used to calibrate the models. Any

* E-mail: ctodd@soest.hawaii.edu

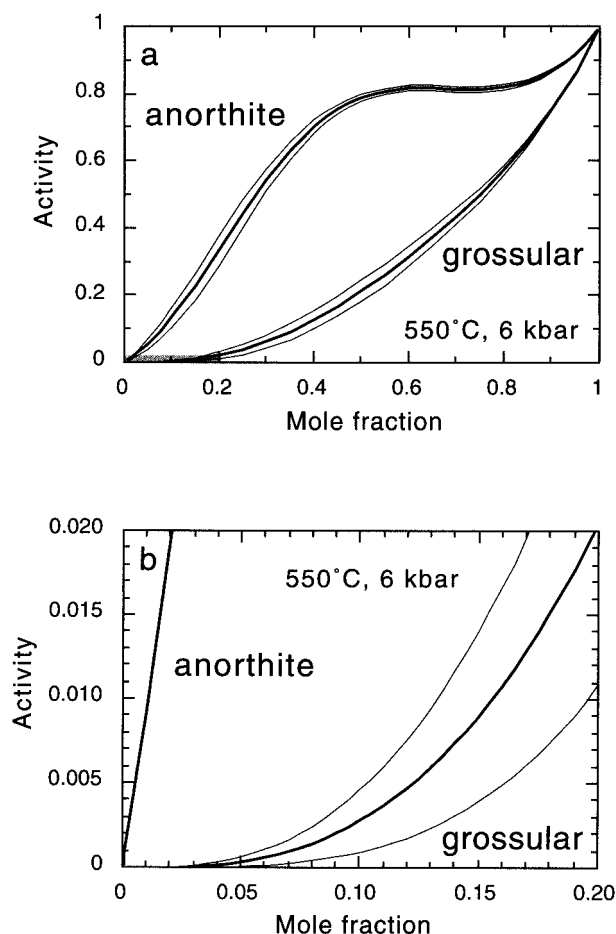


FIGURE 1. (a) Heavy lines show activity as a function of composition for anorthite in plagioclase (Fuhrman and Lindsley 1988) and grossular in garnet (Berman 1990) at 550 °C and 6 kbar. Plagioclase contains no K; garnet contains no Mn and Mg/(Mg + Fe) remains fixed at 0.2. Light lines show one standard deviation in activity based on the model of Powell and Holland (1988) (Eq. 1). (b) Enlargement of low mole fraction area shown as a gray box in top diagram. No error envelope is shown for anorthite in b because Equation 1 does not apply if mole percent < 3.

activity model, no matter how well calibrated, is likely to have a larger relative error at low mole fraction than at high mole fraction. Powell and Holland (1988) proposed that for mole fractions greater than ~0.03 the absolute error in activity ($\sigma_{\text{activity}}^{\text{mineral}}$) is

$$\sigma_{\text{activity}}^{\text{mineral}} = 0.3na(1 - \sqrt[n]{a})^2 \quad (1)$$

where a is activity and n is the site multiplicity of the dominant site involved in the solid solution (i.e., 1 for plagioclase and 3 for pyroxene garnets). This equation is based on the propagation of an error in a regular solution energy term (Margules parameter) into the formula for the activity of a one-site mineral. Although this is not a rigorous propagation for the specific irregular solution

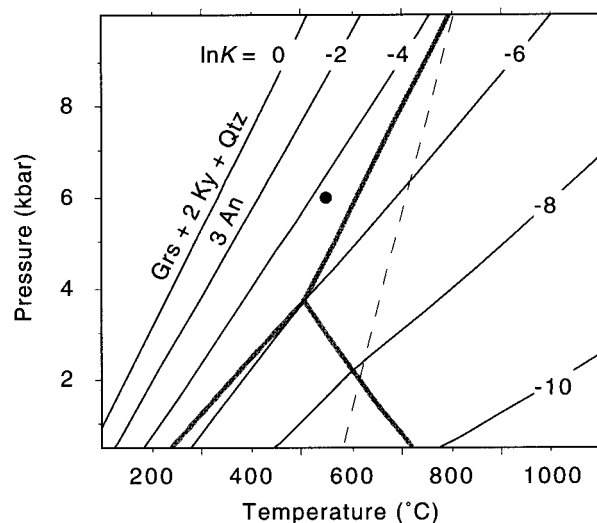


FIGURE 2. Pressure-temperature diagram showing $\ln K$ isopleths of the GASP barometer. Dashed line is α - β quartz transition. Thick gray lines are aluminosilicate equilibria. Conditions discussed in the text (550 °C, 6 kbar) shown as filled circle.

models used here, the functional form takes account of the major effect. A comparison of activity coefficients calculated by a number of different solution models for garnet and plagioclase shows that relative discrepancies among models increase as mole fraction decreases (Kohn and Spear 1991b), supporting the trend implied by Equation 1. Figure 1 shows the standard deviation around the activities of anorthite and grossular at 550 °C and 6 kbar as a function of mole fraction based on the solution models of Fuhrman and Lindsley (1988) and Berman (1990), respectively. For these calculations the plagioclase contains no K, and the garnet contains no Mn with Mg/(Mg + Fe) fixed at 0.2.

The effect that uncertainty in activity has on the pressure determined by the GASP barometer can be calculated directly. The GASP barometer is located in P - T space according to the equation, $0 = \Delta G_r^0 + \int_{1\text{bar}, 298\text{K}}^{P, T} (\Delta V_r dP - \Delta S_r dT) + RT \ln K$, where ΔG_r^0 is the free energy difference of the pure end-members at standard-state conditions, ΔV_r the volume difference, ΔS_r the entropy difference, and K the equilibrium constant of the reaction. In this case, $K = (a_{\text{grs}} a_{\text{Ky}}^2 a_{\text{Qtz}}) / (a_{\text{an}}^3) = a_{\text{grs}} / a_{\text{an}}^3$, where a_{mineral} is the activity of the mineral species indicated and $a_{\text{Ky}} = a_{\text{Qtz}} = 1$. The relationship between P , T , and $\ln K$ is shown in Figure 2 using the thermodynamic database from Berman (1988). At constant T , the uncertainty in a mineral activity (Eq. 1) propagates into P according to

$$\sigma_P^{\text{activity}} = \left(\frac{\partial P}{\partial \ln K} \right)_T \left(\frac{\partial \ln K}{\partial a_{\text{mineral}}} \right) \sigma_{\text{activity}}^{\text{mineral}} \quad (2)$$

The derivative $\partial P / \partial \ln K$ at 550 °C and 6 kbar is 1.08 kbar/ $\ln K$ (Fig. 2). The derivatives of $\ln K$ are $1/a_{\text{grs}}$ and $-3/a_{\text{an}}$ for grossular and anorthite, respectively. It is assumed that $\sigma_{\text{activity}}^{\text{Qtz}} = \sigma_{\text{activity}}^{\text{Ky}} = 0$.

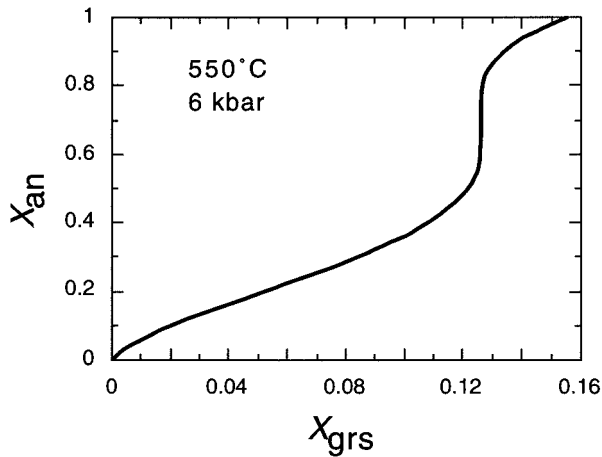


FIGURE 3. X_{an} vs. X_{grs} for the assemblage Grt + Pl + Qtz + Ky at 550 °C, 6 kbar. The same compositional constraints apply as in Figure 1. These data were calculated by: (1) setting the garnet composition; (2) solving for grossular activity (Berman 1990); (3) solving for anorthite activity from $K = 0.01 = a_{grs}/a_{an}^3$; and then (4) solving for the composition of plagioclase (Fuhrman and Lindsley 1988) iteratively.

Solution models relate composition to activity. At fixed P and T , the equilibrium constant for GASP relates the two activities; $a_{grs}/a_{an}^3 \approx 0.01$ at 550 °C and 6 kbar. For a hypothetical outcrop equilibrated under these conditions, a series of rocks can be postulated having the same assemblage (Grt + Ky + Qtz + Pl) but different bulk Ca-contents, and therefore different X_{grs} and X_{an} . Figure 3 shows the relationship of X_{grs} to X_{an} at this hypothetical outcrop based on the given equilibrium constant and the activity models depicted in Figure 1. Figure 4 shows $\sigma_P^{activity}$ as a function of X_{grs} . As can be seen, $\sigma_P^{activity}$ is larger at low values of mole fraction. At $X_{grs} = 0.03$ and $X_{an} = 0.133$, σ_P from grossular and anorthite activities are 0.89 and 0.63 kbar, respectively, whereas at $X_{grs} = 0.15$ and $X_{an} = 0.98$ they are 0.61 and 0.00 kbar. The uncertainty in P from grossular activity is always larger than that from anorthite activity.

Uncertainty in composition determination

There is a limit to how well one can know the composition of a mineral that was in equilibrium with the rest of the metamorphic assemblage at the specific time of metamorphism of interest. The sources of uncertainty include compositional zoning, inhomogeneity on the scale of a thin section, retrogression, and analytical error from the microprobe. Rather than addressing each of these uncertainties individually, they are treated together. The ultimate impact is an uncertainty in the appropriate composition. This value is likely to be different for different samples. Therefore there is no single optimal value. A minimal estimate is ± 1 mol% ($\sigma_{composition}^{mineral} = 0.01$). Keep in mind that this is meant to represent the sum total of all uncertainties in composition. An uncertainty in compo-

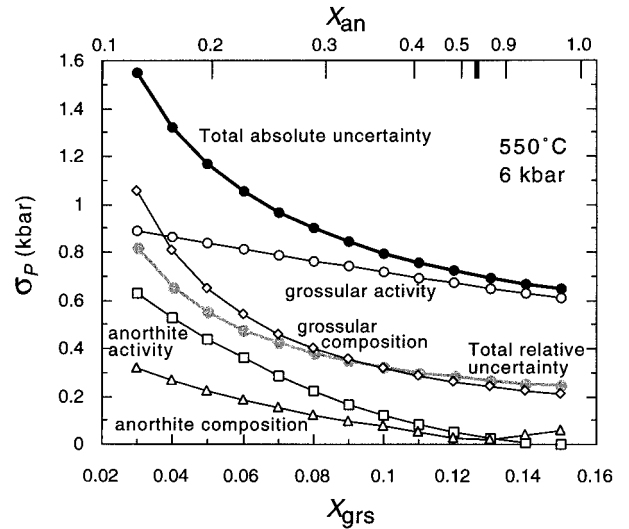


FIGURE 4. Standard deviation in pressure as a function of X_{grs} for the assemblage Grt + Pl + Qtz + Ky at 550 °C, 6 kbar and the compositional constraints in Figure 1. Each of the four individual absolute uncertainties described in the text are shown, as well as the total absolute uncertainty. Gray line is total relative uncertainty. Shown along the top of the diagram is the corresponding X_{an} from Figure 3.

sition affects the uncertainty in P calculated by the GASP barometer according to

$$\sigma_P^{composition} = \left(\frac{\partial P}{\partial \ln K} \right)_T \left(\frac{\partial \ln K}{\partial a_{mineral}} \right) \left(\frac{\partial a_{mineral}}{\partial X_{mineral}} \right) \sigma_{composition}^{mineral} \quad (3)$$

where the derivatives $\partial a_{mineral}/\partial X_{mineral}$ were solved by fitting a polynomial to activity vs. composition data from activity models for the composition range of interest. Figure 4 shows $\sigma_P^{composition}$ as a function of X_{grs} for the same set of hypothetical rocks as described in the previous section. At $X_{grs} = 0.03$ and $X_{an} = 0.133$, σ_P from grossular and anorthite mole fraction uncertainties is 1.05 and 0.32 kbar, respectively, whereas at $X_{grs} = 0.15$ and $X_{an} = 0.98$, $\sigma_P^{composition}$ is 0.21 and 0.06 kbar, respectively. Uncertainty estimates for a different choice of $\sigma_{composition}^{mineral}$ are easily calculated by substituting this new value into Equation 3. For all possible compositions at these P - T conditions, $\sigma_P^{composition}$ is dominated by the uncertainty in the grossular term, as also noted by Hodges and McKenna (1987). The minimum in uncertainty from anorthite composition at $X_{grs} = 0.13$ is caused by the near zero slope of a_{an} vs. X_{an} in this portion of P - T -composition space (Fig. 1).

Combined effect

If all four sources of the uncertainties in P discussed above are uncorrelated ($\sigma_{activity}^{grs}$, $\sigma_{activity}^{an}$, $\sigma_{composition}^{grs}$, $\sigma_{composition}^{an}$), the total uncertainty in pressure is the square root of the sum of the squares of the individual uncertainties in P . Since activity models for garnet and plagioclase were determined from independent sets of data, the covariance is zero for errors in a_{grs} and a_{an} . The error from an activity

model is most likely systematic and comes from the modeler's choice of functional form and data set used. Composition errors have both random and systematic parts. Random compositional errors would be those associated with counting statistics from the microprobe and mineral inhomogeneity. Systematic compositional errors come from the choice of microprobe standards, and perhaps zoning (which point on a zoning profile is chosen). There is no correlation between an error in an activity model and the error in measuring composition. Therefore covariance is zero for activity-composition pairs. The only errors that might be correlated are $\sigma_{\text{composition}}^{\text{grs}}$ and $\sigma_{\text{composition}}^{\text{an}}$. The uncertainty from microprobe counting statistics and the amount of zoning or compositional heterogeneity in these two minerals is not necessarily correlated, but there is a high covariance between the systematic part of microprobe errors for samples measured in a single lab. However, if the amount of uncertainty from zoning, compositional heterogeneity, and microprobe counting statistics is greater than that from systematic microprobe errors, the assumption of uncorrelated compositional uncertainties is deemed justified. Thus the combined uncertainty in pressure determination from all four sources ranges from 0.65 kbar at high mole fractions to 1.55 kbar at low mole fractions (Fig. 4). The relatively large uncertainty even at Ca-rich conditions comes mostly from the uncertainty inherent in grossular activity (89% of the variance), with almost all of the remaining variance (10%) coming from the uncertainty in the composition of garnet. At Ca-poor conditions, the uncertainty is distributed more evenly, although it remains dominated by grossular terms ($\sigma_{\text{activity-grs}}^{\text{grs}}$ contains 33% of the variance, $\sigma_{\text{compos-grs}}^{\text{compos-grs}}$ 46%, $\sigma_{\text{activity-an}}^{\text{activity-an}}$ 16%, $\sigma_{\text{compos-an}}^{\text{compos-an}}$ 4%).

The uncertainties presented above are meant to represent absolute uncertainties in determining the P - T of equilibration of a rock. For relative errors, uncertainties would be smaller. In particular, the uncertainties stemming from activity models should be reduced to about one third of that calculated by Equation 1 (Powell and Holland 1988). Relative errors from the microprobe would likewise be greatly reduced, but compositional uncertainty from zoning and inhomogeneity remains the same. The net result on the total uncertainty is shown as the gray line in Figure 4 for the case where activity uncertainties are multiplied by one third and compositional uncertainties are multiplied by two thirds. At high mole fractions the total relative uncertainty is 0.25 kbar, increasing to 0.82 kbar at low mole fractions.

Different P - T conditions or compositional constraints

The previous calculations are based on specific P - T and mineral composition constraints. One way of deciphering the effect that different input parameters have on σ_p is to examine the constituent parts of Equations 2 and 3. Figure 2 shows that $(\partial P/\partial \ln K)_p$, common to both equations, is a function of T , ranging over a factor of two, from 0.8 kbar/ $\ln K$ at 350 °C to 1.8 kbar/ $\ln K$ at 850 °C. It is not affected by composition change. As mentioned above,

$(\partial \ln K/\partial a_{\text{mineral}})$ is fixed by the stoichiometry of the equilibrium and is a function of the inverse of activity. The activity of grossular is affected both by composition and P - T change. Increasing Mg/(Mg + Fe) in garnet from 0 to 0.5 increases the activity of grossular for a specific X_{grs} less than a factor of three. Pressure has little impact on activity, but activity doubles for a given composition from 800 to 400 °C. Equation 1 shows that $\sigma_{\text{activity}}^{\text{grs}}$ also is a function of a_{grs} . The result of decreasing T and increasing Mg as before on $\sigma_{\text{activity}}^{\text{grs}}$ is up to a factor of six increase, especially at low mole fractions. The net result of all these factors is that the greatest increase of $\sigma_p^{\text{activity-grs}}$ at a given grossular content is from Mg-rich low- T to Fe-rich high- T conditions, changing by up to a factor of five. For the field example presented in the next section Mg/(Mg + Fe) varies only from 0.1 to 0.2, and T differs over only 200 °C, leading to at most a factor of two change in theoretical calculations.

As argued in a previous section, $\sigma_{\text{composition}}^{\text{mineral}}$ is a function of sample heterogeneity and analytical technique, and therefore not a function of P - T or mineral composition. A change in pressure has an insignificant effect on $(\partial a_{\text{grs}}/\partial X_{\text{grs}})$ but a change from 800 to 400 °C increases it by up to a factor of three. A change in Mg/(Mg + Fe) in garnet from 0.1 to 0.5 increases this derivative by up to an order of magnitude. The net result is that $\sigma_p^{\text{compos-grs}}$ can increase up to a factor of five from low- T Fe-rich to high- T Mg-rich compositions. However, for more modest ranges of T and composition, as discussed earlier, $\sigma_p^{\text{compos-grs}}$ may increase up to a factor of two.

Except at high temperatures, the K content of plagioclase is very low. This small compositional change has an insignificant effect on calculated results. Different P - T conditions can cause a change in K (Fig. 2), leading to a different a_{an} , $(\partial \ln K/\partial a_{\text{an}})$, $\sigma_{\text{activity}}^{\text{an}}$, and $(\partial a_{\text{an}}/\partial X_{\text{an}})$ for a given garnet composition. In effect, the change in K from low P / T to high P / T leads to stretching of the X axis of the anorthite components in Figure 4. This increase in $\sigma_p^{\text{activity-an}}$ and $\sigma_p^{\text{compos-an}}$ for a given garnet composition is partly balanced by a decrease caused by $(\partial P/\partial \ln K)_T$ noted above.

Considering all factors, high P / T Fe-rich conditions increase $\sigma_p^{\text{compos-an}}$ and $\sigma_p^{\text{activity-an}}$ and decrease $\sigma_p^{\text{compos-grs}}$ and $\sigma_p^{\text{activity-grs}}$. Each constituent part of σ_p changes by less than a factor of two for modest changes in P - T (2 kbar, 200 °C) and composition [0.1 Mg/(Mg + Fe)]. The distribution of variance between the components of σ_p changes, but the inverse relationship of σ_p and X_{grs} is robust. Calculations using other Ca-bearing equilibria (GRIPS, GMAP, etc.) are different in detail, but also preserve the inverse relationship of σ_p and X_{grs} .

NATURAL SAMPLES

To test the applicability of the preceding theoretical calculations it is necessary to have an independent data set that includes the error of a pressure estimate and the mole fraction of grossular and anorthite. Ideally, all samples would have equilibrated under the same P - T and

TABLE 1. Sample list and *P-T* results

Sample name	X_{grs}	X_{an}	Including Ca-minerals		Excluding Ca-minerals		Assemblage used* (All contain Grt Bt Pl Qtz)
			<i>T</i> (°C)	<i>P</i> (kbar)	<i>T</i> (°C)	<i>P</i> (kbar)	
Al378	0.043	0.154	576	6.55	587	5.23	Ms Ky
Al405	0.061	0.187	538	5.76	576	4.43	Ms Sil
B367	0.043	0.250	703	6.70	706	6.45	Ms Sil
BG8810	0.064	0.116	558	8.75	635	6.46	Ilm Rt
DS05	0.038	0.267	682	4.83	682	4.38	Ms Sil
DS07	0.035	0.156	615	6.63	600	7.03	Ilm Rt Ky
DS08	0.038	0.202	608	5.68	576	6.62	Ilm Rt Ky
DS10	0.033	0.245	620	4.28	622	5.00	Ms Sil
EF736	0.162	0.528	587	7.40	581	8.19	Ms Ky
EF741	0.171	0.471	590	7.71	587	7.71	Ms Ky
EF806	0.210	0.661	445	5.32	442	5.56	Ms Ky
EK45	0.032	0.216	600	3.93	601	3.68	Ms Sil
KL185	0.058	0.236	570	5.62	571	5.33	Ms Ky
KL437	0.071	0.214	682	8.14	693	6.02	Ms Sil
Ma9302	0.205	0.677	411	4.78	402	4.80	Ms Ilm Rt
Ma9307c	0.212	0.786	476	5.55	490	5.25	Ms Ilm Rt
Ma9330	0.139	0.134	534	8.45	616	6.18	Ms Ilm Rt Ky
Ma9415	0.059	0.288	588	5.41	594	6.15	Ms Ilm Rt Sil
Ma9418	0.070	0.226	560	6.34	595	5.02	Ms Sil
Ma9422	0.039	0.219	578	4.61	578	4.58	Ms Sil
Ma9437	0.064	0.166	609	7.92	615	7.53	Ms Ilm Rt
Ma9450	0.085	0.232	604	7.64	656	6.40	Ms Ilm Rt Ky
Ma9464	0.176	0.445	502	5.67	508	5.30	Ms Ilm Rt Ky
Ma9477	0.150	0.230	577	9.08	601	6.14	Ms Ky
Ma9506	0.048	0.261	658	5.98	657	5.55	Ms Sil
Mag096	0.045	0.249	617	5.41	617	6.42	Ms Ilm Rt Ky
Mag193	0.051	0.337	610	6.65	628	4.91	Ilm Rt Ky
NW076	0.074	0.300	545	5.16	542	6.48	Ms Ky
NW077	0.096	0.167	554	8.21	585	4.32	Ms Ky
RT159	0.046	0.196	564	5.66	563	6.06	Ms Ky
Si9403	0.173	0.413	599	8.15	604	6.98	Ms Ky
Si9414	0.069	0.222	589	6.96	616	6.22	Ms Ilm Rt Ky
Si9503	0.060	0.266	573	5.50	564	6.89	Ms Ky
Staps012	0.137	0.220	511	7.30	523	5.08	Ms Ky
Staps025	0.088	0.205	543	7.05	545	6.36	Ms Ky
Staps038	0.067	0.109	539	8.72	558	6.38	Ms Ky
Staps077	0.061	0.156	556	7.31	567	5.54	Ms Ky
T022	0.080	0.242	568	6.58	580	5.18	Ms Ky
T031	0.035	0.174	600	5.89	587	6.34	Ms Ilm Rt Ky
TT379	0.101	0.191	566	8.38	577	6.41	Ms Ky
TT479	0.125	0.324	576	7.29	553	9.10	Ms Ky
TT480	0.153	0.396	540	6.47	548	4.78	Ms Ky

Note: Abbreviated compositions are listed in Todd and Engi (1997) and Engi et al. (1995). Complete mineral compositions can be obtained from the author.

* Mineral abbreviations from Kretz (1983).

have identical compositional constraints on non-Ca components. Such a database is not available, but the preceding section indicates that the theoretical calculations still apply in a field area with modest ranges of *P* and *T* (~2 kbar, ~200 °C). For natural samples, it is not possible to directly measure the error of a pressure estimate because this would require that the “true” pressure of equilibration is known. An estimate of this error, independent of theoretical calculations, comes from the comparison of *P* estimates from anorthite-grossular-bearing equilibria to *P* estimates that do not use these components.

A subset of amphibolite grade metapelitic rocks in the Central Alps, described by Todd and Engi (1997) and Engi et al. (1995), was investigated. Of the 110 samples used in their work, 42 have mineral assemblages appropriate for the purpose of this paper. Thermobarometry indicates a *P-T* range of 4.5–7 kbar and 500–675 °C. For each of the samples the *P-T* of equilibration (both in-

cluding grossular-anorthite-bearing equilibria and excluding these equilibria) was determined by TWQ software (Berman 1991) using the thermodynamic database of Berman (1988). The assemblages examined are mostly Grt + Bt + Ms + Qtz + Pl with either an aluminosilicate or Rt + Ilm, or all three (Table 1). This allows for the calculation of sets of H₂O-conserved equilibria with three or four linearly independent reactions that include the phases grossular + anorthite, which reduces to two or three linearly independent reactions when the Ca-phases are excluded. Assemblages used and *P-T* results are listed in Table 1. Pressures and temperatures of equilibration were estimated in the following manner: for a given sample, all possible stable and metastable equilibria were calculated; the *P-T* values of the intersection of each pair of equilibria are tabulated, and the weighted average of this table is the *P-T* estimate for the sample. For more information about this technique, see Berman (1991). [For

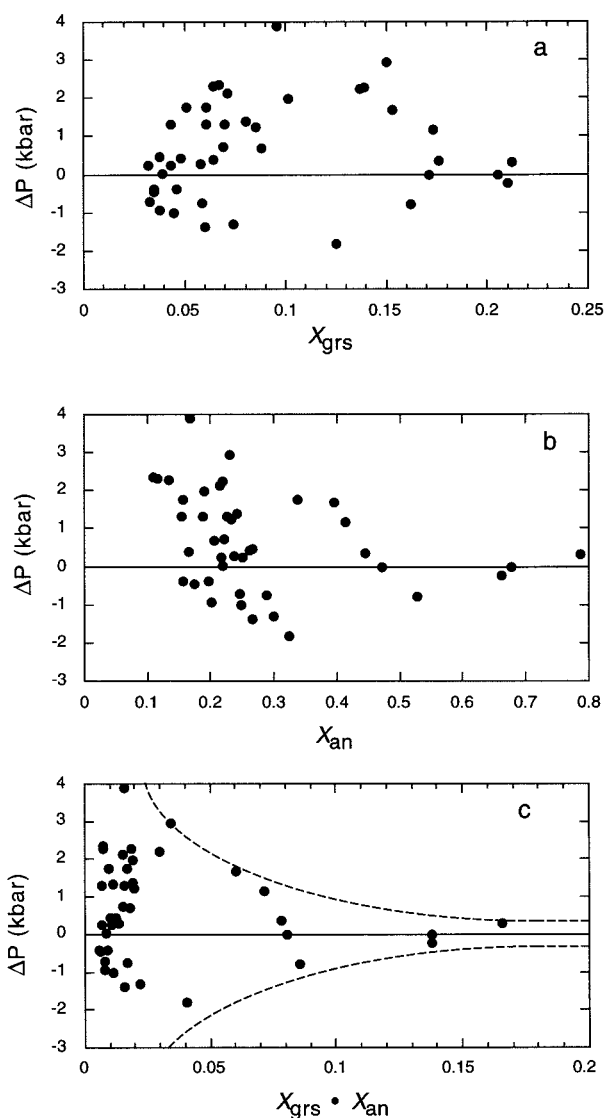


FIGURE 5. ΔP (see text) vs. (a) X_{grs} , (b) X_{an} , and (c) the product $X_{grs} \cdot X_{an}$ for the set of natural samples described in the text. There is a strong inverse relationship between the range in ΔP and $X_{grs} \cdot X_{an}$. (c) also shows interpreted uncertainty envelope.

more details on the samples used, see Engi et al. (1995) and Todd and Engi (1997). Activity models for the minerals are as follows: Alm, Prp and Grs, Berman (1990); An, Fuhrman and Lindsley (1988); Phl and Ann, McMullin et al. (1991); Ms, Chatterjee and Froese (1975); Ilm, ideal.]

Comparison of the two P estimates for each rock gives a measure of how well Ca-bearing equilibria (GASP, GRIPS, GMAP, and the family of dependent reactions spawned by intersections of these with the other equilibria in the system) agree with non-Ca-bearing equilibria. Because these rocks span a range in grossular and anorthite mole fractions they can be used to examine this agreement as a function of mole fraction. In these sam-

ples the difficulty of low mole fraction is mostly confined to grossular and anorthite. Almost all the non-Ca-bearing mineral end-members used (alm, prp, ann, phl, ms, ilm, Qtz, Rt, Ky, Sil) have higher mole fractions than grossular; only X_{prp} is less than X_{grs} in nine out of 42 samples. In most cases the non-Ca-bearing end-members have a higher mole fraction than anorthite as well: $X_{an} > X_{alm}$ in one sample; $X_{an} > X_{ms}$ in two; $X_{an} > X_{phl}$ in four; $X_{an} > X_{ann}$ in 10; $X_{an} > X_{prp}$ in 40; X_{ilm} is in all cases greater than X_{an} ; quartz, rutile, and aluminosilicate were assumed to be pure.

Figures 5a and 5b show the pressure estimate from assemblages including Ca-bearing equilibria minus that derived from the same assemblages without the Ca-bearing equilibria (ΔP) as a function of X_{grs} and X_{an} . There is an inverse relationship between X_{an} and the range in ΔP , but no clear functionality appears between X_{grs} and ΔP . In order to examine ΔP in relation to grossular and anorthite content simultaneously, Figure 5c shows ΔP as a function of the product $X_{grs} \cdot X_{an}$. Similar to Figure 5b, there is a strong inverse correlation between the range in ΔP and $X_{grs} \cdot X_{an}$. This is interpreted to indicate that although the accuracy of P estimates at low grossular and anorthite contents remains high in comparison with independent estimates, precision is low. It is suggested that if the product $X_{grs} \cdot X_{an}$ is below 0.05, pressure estimates from grossular-anorthite-bearing equilibria in metapelites should be used only with great caution.

ACKNOWLEDGMENTS

Helpful reviews of an earlier version of this paper were kindly provided by D.L. Whitney and B.W. Evans. Journal reviews by D. Henry and L.W. McKenna III also improved the paper.

REFERENCES CITED

- Anderson, G.M. (1977a) The accuracy and precision of calculated mineral dehydration equilibria. In D.G. Fraser, Ed., *Thermodynamics in Geology*, 115–136. Reidel, Boston.
- (1977b) Uncertainties in calculations involving thermodynamic data. In H.J. Greenwood, Ed., *Applications of Thermodynamics to Petrology and Ore Deposits*, MAC Short Course, 199–214. Love, Ottawa.
- Applegate, J.D.R. and Hodges, K.V. (1994) Empirical evaluation of solution models for pelitic minerals and their application to thermobarometry. *Contributions to Mineralogy and Petrology*, 117, 56–65.
- Berman, R.G. (1988) Internally-consistent thermodynamic data for minerals in the system $\text{Na}_2\text{O}-\text{K}_2\text{O}-\text{CaO}-\text{MgO}-\text{FeO}-\text{Fe}_2\text{O}_3-\text{Al}_2\text{O}_3-\text{SiO}_2-\text{TiO}_2-\text{H}_2\text{O}-\text{CO}_2$. *Journal of Petrology*, 29, 445–522.
- (1990) Mixing properties of Ca-Mg-Fe-Mn garnets. *American Mineralogist*, 75, 328–352.
- (1991) Thermobarometry using multi-equilibrium calculations: a new technique, with petrological applications. *Canadian Mineralogist*, 29, 833–855.
- Bohlen, S.R. and Liotta, J.J. (1986) A barometer for garnet amphibolites and garnet granulites. *Journal of Petrology*, 27, 1025–1034.
- Chatterjee, N.D. and Froese, E.F. (1975) A thermodynamic study of the pseudobinary join muscovite-paragonite in the system $\text{KAISi}_3\text{O}_8-\text{NaAlSi}_3\text{O}_8-\text{Al}_2\text{O}_3-\text{SiO}_2-\text{H}_2\text{O}$. *American Mineralogist*, 60, 985–993.
- Engi, M., Todd, C.S., and Schmatz, D.R. (1995) Tertiary metamorphic conditions in the eastern Lepontine Alps. *Schweizerische Mineralogische und Petrographische Mitteilungen*, 75, 347–369.
- Fuhrman, M.L. and Lindsley, D.H. (1988) Ternary-feldspar modeling and thermometry. *American Mineralogist*, 73, 201–215.

- Ghent, E.D. (1976) Plagioclase-garnet- Al_2SiO_5 -quartz: a potential geobarometer-geothermometer. *American Mineralogist*, 61, 710–714.
- Ghent, E.D. and Stout, M.Z. (1981) Geobarometry and geothermometry of plagioclase-biotite-garnet-muscovite assemblages. *Contributions to Mineralogy and Petrology*, 76, 92–97.
- Gordon, T.M. (1992) Generalized thermobarometry: Solution of the inverse chemical equilibrium problem using data for individual species. *Geochimica et Cosmochimica Acta*, 56, 1793–1800.
- Gordon, T.M., Aronovich, L.Y., and Fed'kin, V.V. (1994) Exploratory data analysis in thermobarometry: An example from the Kisseynew sedimentary gneiss belt, Manitoba, Canada. *American Mineralogist*, 79, 973–982.
- Hodges, K.V. and Crowley, P.D. (1985) Error estimation and empirical geothermobarometry for pelitic systems. *American Mineralogist*, 70, 702–709.
- Hodges, K.V. and McKenna, L.W. (1987) Realistic propagation of uncertainties in geologic thermobarometry. *American Mineralogist*, 72, 671–680.
- Kohn, M.J. and Spear, F.S. (1991a) Error propagation for barometers: 1. Accuracy and precision of experimentally located end-member reactions. *American Mineralogist*, 76, 128–137.
- (1991b) Error propagation for barometers: 2. Application to rocks. *American Mineralogist*, 76, 138–147.
- Kretz, R. (1983) Symbols for rock-forming minerals. *American Mineralogist*, 68, 277–279.
- Lieberman, J. and Petrakakis, K. (1991) TWEEQU thermobarometry: Analysis of uncertainties and application to granulites from western Alaska and Austria. *Canadian Mineralogist*, 29, 857–887.
- McKenna, L.W. and Hodges, K.V. (1988) Accuracy versus precision in locating reaction boundaries: Implications for the garnet-plagioclase-aluminum silicate-quartz geobarometer. *American Mineralogist*, 73, 1205–1208.
- McMullin, D., Berman, R.G., and Greenwood, H.J. (1991) Calibration of the SGAM thermobarometer for pelitic rocks using data from phase equilibrium experiments and natural assemblages. *Canadian Mineralogist*, 29, 889–908.
- Powell, R. and Holland, T. (1994) Optimal geothermometry and geobarometry. *American Mineralogist*, 79, 120–133.
- Powell, R. and Holland, T.J.B. (1988) An internally consistent thermodynamic dataset with uncertainties and correlations: 3. Applications to geobarometry, worked examples and a computer program. *Journal of Metamorphic Geology*, 6, 173–204.
- Todd, C.S. and Engi, M. (1997) Metamorphic Field Gradients in the Central Alps. *Journal of Metamorphic Geology*, 15, 513–530.

MANUSCRIPT RECEIVED SEPTEMBER 8, 1997

MANUSCRIPT ACCEPTED JULY 3, 1998

PAPER HANDLED BY DAVID W. MOGK